https://doi.org/10.5194/amt-2020-365
Preprint. Discussion started: 12 November 2020
© Author(s) 2020. CC BY 4.0 License.

Atmospheric Measurement Techniques Discussions

Simultaneous measurement of $\delta^{13}C$, $\delta^{18}O$ and $\delta^{17}O$ of atmospheric CO_2 - Performance assessment of a dual-laser absorption spectrometer

Pharahilda M. Steur[1], Hubertus A. Scheeren[1], Dave D. Nelson[2], J. Barry McManus[2], and Harro A. J. Meijer[1]

[1]Centre for Isotope Research, University of Groningen, Nijenborgh 6, 9747 AG Groningen, The Netherlands
[2]Aerodyne Research Inc., 45 Manning Road, Billerica, MA 01821-3976, USA

Correspondence: P.M. Steur (p.m.steur@rug.nl)

Abstract. Using laser absorption spectrometry for the measurement of stable isotopes of atmospheric CO_2 instead of the traditional Isotope Ratio Mass Spectrometry (IRMS) method decreases sample preparation time significantly, and uncertainties in the measurement accuracy due to CO_2 extraction and isobaric interferences are avoided. In this study we present the measurement performance of a new dual-laser instrument developed for the simultaneous measurement of the $\delta^{13}C$, $\delta^{18}O$ and $\delta^{17}O$ of atmospheric CO_2 in discrete air samples, referred to as the Stable Isotopes of CO_2 Absorption Spectrometer (SICAS). We compare two different calibration methods: the ratio method (RM) based on measured isotope ratio and a CO_2 mole fraction dependency correction (CMFD), and the isotopologue method (IM) based on measured isotopologue abundances. Calibration with the RM and IM is based on three different assigned whole air references calibrated on the VPBD scale. An additional quality control tank (QC) is included in both methods to follow long-term instrument performance. Measurements of the QC tank show that best performance is achieved with the RM for both the $\delta^{13}C$ and $\delta^{18}O$ measurements with mean residuals of 0.007‰ and 0.016‰ and mean standard errors of 0.009‰ and 0.008‰ respectively, during periods of optimal measurement conditions. The $\delta^{17}O$ standard error in the same measurement period is 0.013‰. In addition, intercomparing a total of 14 different flask samples covering a CO_2 mole fraction range of 344-439 ppm with the Max Planck Institute for Biogeochemistry shows a mean residual of 0.002‰ and a standard deviation of 0.063‰ for $\delta^{13}C$, using the RM. The $\delta^{18}O$ could not be compared due to depletion of the $\delta^{18}O$ signal in our sample flasks because of too long storage times. Finally, we evaluated the potential of our $\Delta^{17}O$ measurements as a tracer for Gross Primary Production (GPP) by vegetation through photosynthesis. Here, a measurement precision of $<$0.01‰ would be a prerequisite for capturing seasonal variations in the $\Delta^{17}O$ signal. So far, a mean standard error of 0.016‰ was achieved for $\Delta^{17}O$ measurements of our QC tank using the RM. Improvements in our measurement procedure, spectral fit and $\delta^{17}O$ calibration are due to reach the required precision.

1 Introduction

As atmospheric CO_2 (atm-CO_2) is the most important contributor to anthropogenic global warming, keeping track of its sources and sinks is essential for understanding and predicting the consequences of climate change for natural systems and

https://doi.org/10.5194/amt-2020-365
Preprint. Discussion started: 12 November 2020
© Author(s) 2020. CC BY 4.0 License.

Atmospheric Measurement Techniques Discussions

societies, and for assessing and quantifying the possible mitigating measures. The stable isotope (si) composition of atm-CO_2 is often used as an additional tool to distinguish between anthropogenic emissions and the influence of the biosphere on varying CO_2 mole fractions (Pataki et al., 2003; Zhou et al., 2005). For this reason, the si composition of atm-CO_2 is monitored at a considerable number of atmospheric measurement stations around the globe. Due to the large size of the carbon reservoir of the atmosphere and high mixing ratios, the effects of sources and sinks on the atmospheric composition are heavily diluted. Changes in the isotope composition of atm-CO_2 are therefore relatively small compared to the actual changes in carbon fluxes (IAEA, 2002). Hence, current climate change- and meteorological research, as well as the monitoring of CO_2 emissions, require accurate and precise greenhouse gas measurements that can meet the WMO/GAW inter-laboratory compatibility goals of 0.01‰ for $\delta^{13}C$ and 0.05‰ for $\delta^{18}O$ of atm-CO_2 for the Northern Hemisphere (WMO, 2016).

Traditionally, high precision stable isotope measurements are done using Isotope Ratio Mass Spectrometry (IRMS) (Roelofzen et al., 1991; Trolier et al., 1996; Allison and Francey, 1995) which requires extraction of CO_2 from the air sample before a measurement is possible. This is a time-consuming process wherein very strict, 100% extraction procedures need to be applied to avoid isotope fractionation and to prevent isotope exchange of CO_2 molecules with other gases or water. Extraction of CO_2 from air is a major contributor to both random and systematic scale differences between laboratories and thus complicates the comparison of measurements (Wendeberg et al., 2013). Further, due to the isobaric interferences of both different CO_2 isotopologues and N_2O molecules, which are also trapped with the (cryogenic) extraction of CO_2 from air, corrections need to be applied for the determination of the $\delta^{13}C$ and $\delta^{18}O$ values. Due to the mass interference of the $^{12}C^{17}O^{16}O$ isotopologue with $^{13}C^{16}O^{16}O$ (and to a lesser extent $^{13}C^{17}O^{16}O$ and $^{12}C^{17}O^{17}O$ with $^{12}C^{18}O^{16}O$), the $\delta^{13}C$ results need a correction (usually referred to as "ion correction") that builds upon an assumed fixed relation between $\delta^{17}O$ and $\delta^{18}O$. This assumed relation has varied in the past (Santrock et al., 1985; Allison et al., 1995; Assonov and Brenninkmeijer, 2003; Brand et al., 2010) giving rise to again systematic differences (and confusion) between laboratories. Determination of the $\delta^{17}O$ of CO_2 samples itself using IRMS is extremely complex, due to the mass overlap of the ^{13}C and ^{17}O containing isotopologues, and can only be done using very advanced techniques restricted to just a few laboratories at the moment (see Adnew et al., 2019, and references therein). As the $\delta^{17}O$ in addition to the $\delta^{18}O$ values in atmospheric CO_2 have the potential to be a tracer for gross primary production and anthropogenic emissions (Laskar et al., 2016; Luz et al., 1999; Koren et al., 2019), a less labor-intensive method that would enable to analyze all three stable isotopologues of atm-CO_2 at a sufficient precision would be an asset.

Optical (laser) spectroscopy now offers this possibility following strong developments in recent years especially for the laser light sources, to perform isotopologue measurements showing precisions close to, or even surpassing IRMS measurements (Tuzson et al., 2008; Vogel et al., 2013; McManus et al., 2015). The technique was developed in the 1990s to a level where useful isotope signals could be measured, first on pure compounds such as water vapour (Kerstel et al., 1999), and soon also directly on CO_2 in dry whole air samples (Becker et al., 1992; Murnick and Peer, 1994; Erdélyi et al., 2002; Gagliardi et al., 2003). Extraction of CO_2 from the air can therefore be avoided and smaller sample sizes suffice. Finally, optical spectroscopy is truly isotopologue-specific and is thus free of isobaric interferences. In this paper we present the performance, in terms of precisions and accuracy, of an Aerodyne dual laser optical spectrometer (CW-IC-TILDAS-D) in use since September 2017, for the simultaneous measurement of $\delta^{13}C$, $\delta^{18}O$ and $\delta^{17}O$ of atm-CO_2, which we refer to as "Stable Isotopes of CO_2 Absorption

https://doi.org/10.5194/amt-2020-365
Preprint. Discussion started: 12 November 2020
© Author(s) 2020. CC BY 4.0 License.

Atmospheric Measurement Techniques Discussions

Spectrometer" (SICAS). In this study the instrument performance over time is discussed in chapter 2, followed by an analysis of the CO_2 mole fraction dependency of the instrument. In chapter 3 we report on the actual ways of performing a calibrated measurement using either individual isotopologue measurements or isotope ratios. Finally in chapter 4, whole air measurement results of the SICAS are evaluated for their compatibility with IRMS stable isotope measurements, as well as the usefulness of the triple oxygen isotope measurements for capturing signals of atmospheric CO_2 sources and sinks.

2 Instrument description

2.1 Instrumental set-up

The optical bench as depicted in figure 1 consists (among others) of the two lasers, several mirrors to combine and deflect the laser beams, the optical cell and two detectors. The two interband cascade lasers (ICL) (Nanoplus GmbH, Germany) operate in the mid infrared region (MIR). The isotopologues that are measured are $^{12}C^{16}O_2$, $^{13}C^{16}O_2$, $^{12}C^{16}O^{18}O$ and $^{12}C^{16}O^{17}O$, which from now on will be indicated as 626, 636, 628 and 627 respectively, following the HITRAN database notation (Rothman et al., 2013). Application of a small current ramp causes small frequency variations so the lasers are swept (with a frequency of 1.7kHz) over a spectral range in which ro-vibrational transitions of the isotopologues occur with similar optical depths (Tuzson et al., 2008). Laser 1 operates in the spectral range of 2350 cm-1 (4.25 μm) for measurement of 627 (and 626) and laser 2 operates around 2310 cm-1 (4.33 μm) for the measurement of 626, 636 and 628. The lasers are thermoelectrically (TEC) cooled and stabilized to temperatures of -1.1°C and 9.9°C, respectively. The beams are introduced in a multi-pass aluminum cell with a volume of 0.16 L in which an air sample is present at low pressure (∼50 mBar). The total path length of the laser light is 36 meters.

After passing the cell the lasers are led to a TEC-cooled infrared detector, measuring the signal from the lasers in the spectral range (figure 2). The lasers, optical cell and detectors are all in a housing that is continuously flushed with N_2 gas to avoid any other absorption by CO_2 than from gas in the optical cell. The temperature within and outside the housing is controlled using a re-circulating liquid chiller set at a temperature of 20°C. The absorption spectra are derived by the software TDLWintel (McManus et al., 2005) that fits the measured signal based on known molecular absorption profiles from the HITRAN database (Rothman et al., 2013). On basis of the integration of the peaks at the specific wavelengths, measured pressure and temperature in the optical cell and the constant path length, the isotopologue mole fractions are calculated by the TDLWintel software with an output frequency of 1Hz. For convenience, the default output for the isotopologue mole fractions are scaled for 'the natural abundances' of the 626, 636, 628 and 627 as defined in Rothman et al. (2013), but for obtaining the raw mole fractions this scaling is avoided.

The gas inlet system, depicted in figure 3, is designed to measure discrete air samples in such a way that one can quickly switch between measurements of different samples. There are three inlet ports (11,14 and 18) which are connected to the sample cross at the heart of system (from now on indicated as inlet volume), where a sample is collected at the target pressure of 200± 0.25 mBar before it is connected to the optical cell. One of the inlet ports (11) is connected to a 1/8" VICI multivalve (Valco Instruments) with 15 potential positions for flask samples or cylinders. Switching between VICI ports is automated by using

https://doi.org/10.5194/amt-2020-365
Preprint. Discussion started: 12 November 2020
© Author(s) 2020. CC BY 4.0 License.

Atmospheric Measurement Techniques Discussions

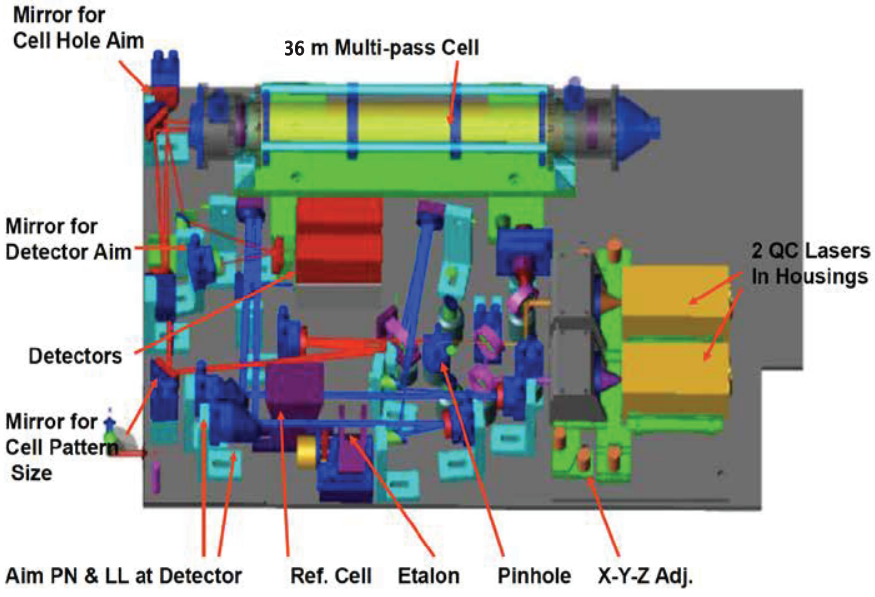

Figure 1. Optical board of the SICAS. (figure adapted from Aerodyne Research, Inc.)

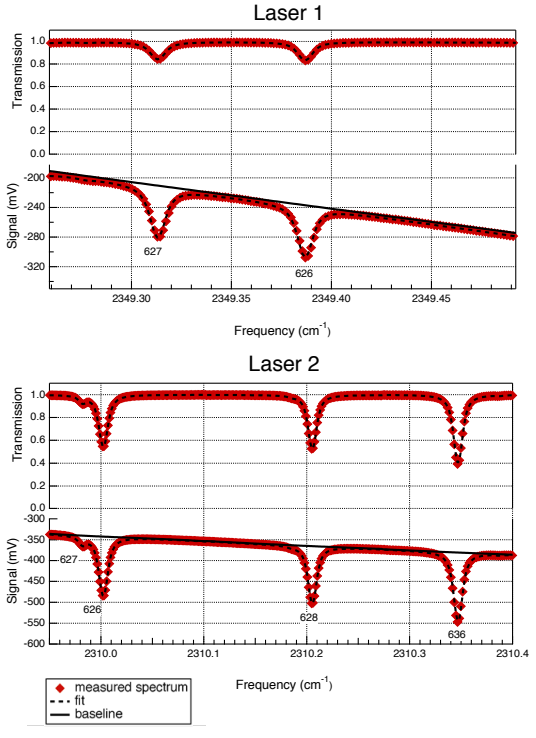

Figure 2. Typical absorption spectrum of laser 1 (top panel) for measurement of 627 and 626, and laser 2 (lower panel) for measurement of 626, 628 and 636.

https://doi.org/10.5194/amt-2020-365
Preprint. Discussion started: 12 November 2020
© Author(s) 2020. CC BY 4.0 License.

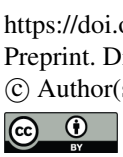

Atmospheric Measurement Techniques Discussions

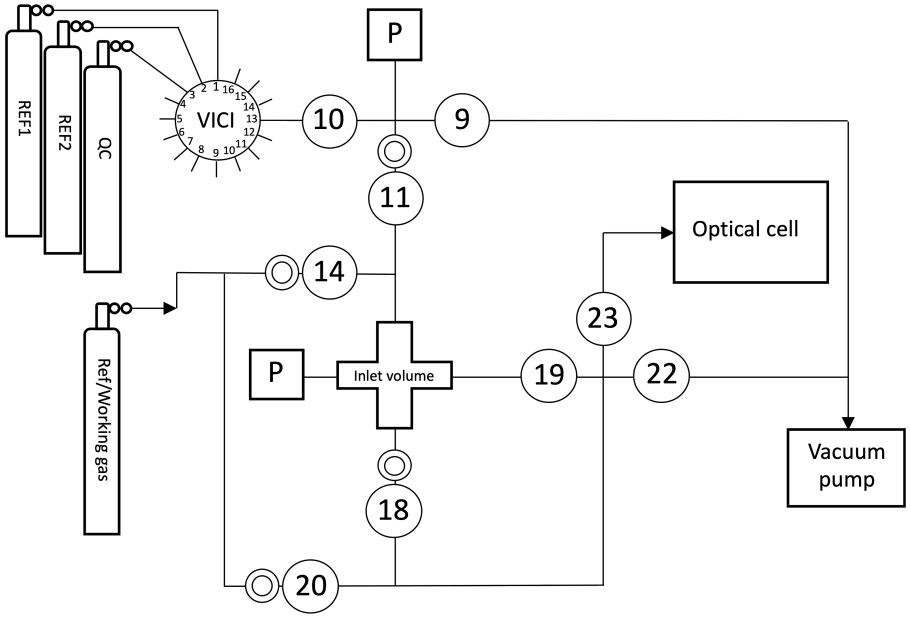

Figure 3. Gas inlet system of the SICAS.

valves 9 and 10 for a flushing procedure to avoid cross contamination in the inlet volume between different samples. A sample gas is led into the inlet volume at reduced flow, as a critical orifice is placed right before the inlet valve, while another gas is being measured inside the optical cell. Since the closing and opening of the valves is controlled by the TDLWintel software, it also controls the duration of the flow into the inlet volume. The target pressure is reached using input from a pressure sensor placed inside the inlet volume. After evacuation of the optical cell (opening valve 22 and 23) the gas from the inlet volume can immediately be brought into the optical cell (opening valve 19 and 23) thereby reducing the sample pressure to ∼50 mBar.

The gas handling procedures are different for measurements of air from cylinders or flasks. For the cylinders, single stage pressure regulators are in use (Rotarex, model SMT SI220), set at an outlet pressure of 600 mBar. If measurements are started after more than two days of inactivity, the internal volume of the regulators is flushed 10 times to prevent fractionation effects. When the VICI valve switches to a cylinder position, the volume between port 10 and 9 is flushed 20 times to prevent memory effects due to the dead volume of the VICI valve.

To open and close the flasks we use a custom-built click-on electromotor valve system (Neubert et al., 2004), making it possible to open the flasks automatically before the measurement. Before opening the flask, the volume between valve 9 and the closed flask is evacuated so there is no need to flush extensively and less sample gas is lost. The actions described above are all steered by a command program developed by Aerodyne Research Inc. called the Switcher program. A bespoke script writing program developed in FileMaker Pro enables us to quickly write scripts for measurement sequences and to directly link those measurements to an internal database.

https://doi.org/10.5194/amt-2020-365
Preprint. Discussion started: 12 November 2020
© Author(s) 2020. CC BY 4.0 License.

Atmospheric Measurement Techniques Discussions

2.2 Instrument performance

The SICAS measurement performance was evaluated by determining the Allan variance of the four measured isotopologue abundances and the three isotope ratios as function of measurement time on a single whole air sample in the sealed optical cell. The isotope ratios, defined as the ratio of the rare isotopologue (636, 628 and 627) and the most abundant 626 isotopologue, are r636, r628 and r627. This experiment was first done in September 2017 and repeated in July 2019 to see the development in time of the measurement precision (figure 4). In all cases, drifts outweigh the averaging process after time periods ranging from 16 seconds to 75 seconds, and this is short compared to the duration of the normal measurement sequences. This is a firm indication that continuous drift correction using a machine working gas is necessary for optimal results.

The precision became significantly worse for all species but isotopologue 627 in the time period between September 2017 and July 2019 due to a gradual but significant decrease (of about 50%) in the measured laser intensity over that period. For most species this led to an increase of the optimal integration time, which is logical given the fact that the minimal precision was higher, such that the increase due to drift influences the acquired precision at a higher integration time, and also at a higher variance level. Figure 4 shows the rapid variance increase due to drift for all isotopologues after less than one minute for the September 2017 measurements, and the same happens for the July 2019 measurements, only less visible due to the higher minimal variance levels.

The decreased laser intensity, leading to a deteriorated signal-to-noise ratio, was caused by contamination of the mirrors in the optical cell, most likely due to precipitation of ultra-fine salt-based aerosols from the sample air occurring during evacuation of the cell. The majority of flask samples measured on the SICAS are from the atmospheric measurement station Lutjewad which is located at the Northern coast of the Netherlands in a rural area dominated by cropland and grassland mainly used for dairy cows. The aerosol composition at Lutjewad is therefore expected to be dominated by sea-salt and ammonium-nitrate from agricultural emissions. Hence, we were able to clean the mirrors and retrieve $\sim 80\%$ of the original laser signal by flushing the mirrors with demi-water and ethanol (in that order). This procedure deviates from the recommended mirror cleaning instructions in which it is advised to use ethanol only to clean the mirrors. The additional use of demi-water was in our case necessary since the precipitated aerosols were not dissolved in ethanol and were therefore not removed when we used ethanol only.

To reduce short-term instrumental drift, all sample measurements needed to be alternated with measurements of a machine working gas, as then the drift corrected signal can be expressed as:

$$M_{S(t)dc} = \frac{M_{S(t)}}{M_{WG(t)}} \quad (1)$$

Where M stands for measurement which can be either the measured isotope ratio or isotopologue abundance, S stands for sample, WG stands for working gas, t stands for time of the sample gas measurement and dc stands for drift corrected. WG(t) is the measured working gas at time t derived from the time-dependent linear regression of the measurements of the working gas bracketing the sample gas measurement. The effectiveness of this drift correction method was tested for both measured isotope ratios and the isotopologue abundances in an experiment in which a tank was measured >10 times alternately with the working gas. For both the isotopologue abundances and isotope ratios the standard deviation was calculated for n=5 and n=10,

https://doi.org/10.5194/amt-2020-365
Preprint. Discussion started: 12 November 2020
© Author(s) 2020. CC BY 4.0 License.

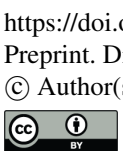

Atmospheric Measurement Techniques Discussions

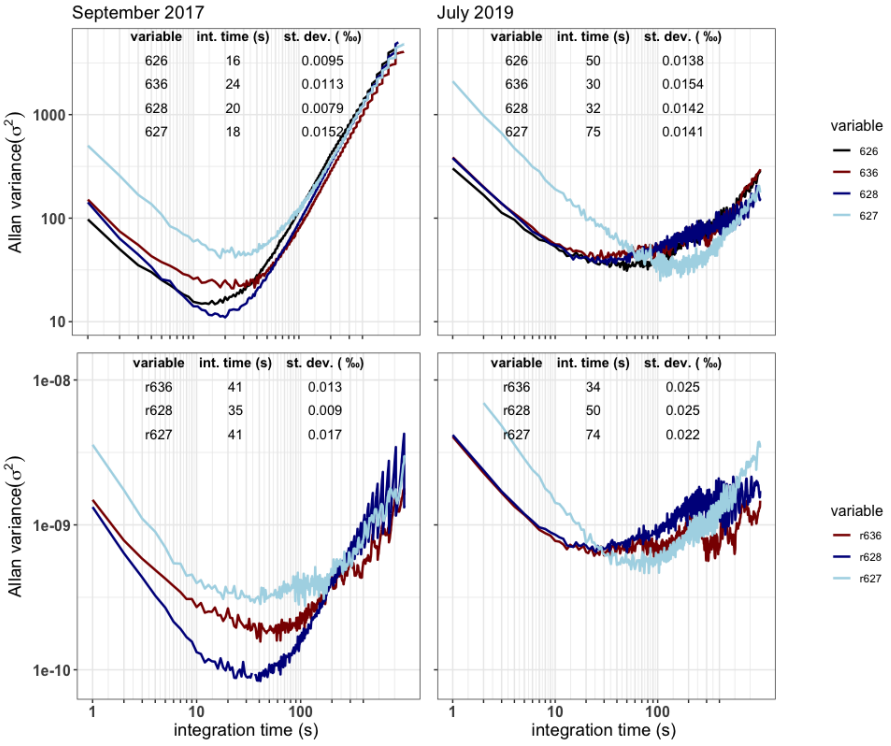

Figure 4. The Allan variance as a function of the integration time in seconds for a single gas measurement plotted for both the measured isotopologue abdundance (top) and the isotope ratios (bottom) at September 2017 (left) and July 2019 (right). The best achieved precisions and corresponding integration times are shown as a table in the plots.

both with and without drift correction (table 1). It is expected that, if the drift correction is effective, the standard deviation does not get worse with a higher n, and that the standard deviations of the uncorrected values are lower than the corrected values.

For the experiment shown in table 1 the standard deviations of the measured isotope ratios are, for both the corrected and the uncorrected values, lower than the standard deviation of the measured isotopologue abundances. The drift correction appears to be less effective for the measured 626 and 628 isotopologue abundances, as the standard deviation of the drift corrected values increases for n=10 compared to n=5 with 0.132 and 0.03 respectively. For the measured isotopologue abundances in general the standard deviations of the corrected values are not always lower than of the uncorrected values. For the measured isotope ratios the drift correction is very effective as the standard deviations of the corrected values are always lower than of the uncorrected values. The increase of the standard deviation between n=5 and n=10 is thereby only between the 0.005 and 0.013‰. We can therefore conclude that the drift correction is more effective for measured isotope ratios than for isotopologue abundances, also resulting in a better repeatability of the isotope ratios compared to the isotopologue abundances.

Cross-contamination, being the dilution of a small volume of the working gas in the sample aliquot that is being measured, and vice versa, as described for a Dual-Inlet IRMS in Meijer et al. (2000), will occur in the SICAS due to the continuous

https://doi.org/10.5194/amt-2020-365
Preprint. Discussion started: 12 November 2020
© Author(s) 2020. CC BY 4.0 License.

Atmospheric Measurement Techniques Discussions

All values	n=5		n=10	
in ‰	uncor	cor	uncor	cor
626	0.121	0.048	0.140	0.180
636	0.126	0.091	0.111	0.077
628	0.089	0.070	0.083	0.100
627	0.066	0.090	0.106	0.072
r636	0.036	0.020	0.055	0.025
r628	0.046	0.021	0.104	0.029
r627	0.060	0.018	0.177	0.031

Table 1. Standard deviations for n=5 and n=10 of uncorrected (uncor) and corrected (cor) isotopologue and isototope ratio measurements. Corrections were done by applying equation 1 on the measurements.

switching between sample and machine working gas. If cross-contamination is not corrected for DI-IRMS measurements inaccuracies can occur when samples of a highly deviating isotope composition are measured. On the SICAS only atmospheric samples are measured that are of very similar isotope values. The CO_2 mole fraction of the samples can deviate quite strongly from the machine working gas, so effects of cross-contamination will have an influence on the CO_2 mole fraction in the optical cell. Experiments show that a fraction between 0.01 and 0.03% of the volume is being diluted in the next sample. A sensitivity analysis was performed and showed that this is such a small amount that scale effects due to cross-contamination are well below the precisions found in this study.

3 Calibration experiments

3.1 The CO_2 mole fraction dependency

The stable isotope composition of atmospheric CO_2 is expressed as a delta value on the VPDB (^{13}C) / VPDB-CO_2 (^{17}O and ^{18}O) scales, which are realized by producing CO_2 gas (using phosphoric acid under well-defined circumstances) from the IAEA-603 marble primary reference material (successor to the now obsolete NBS-19) (IAEA, 2016). A complication when compared to classical DI-IRMS isotope measurements (or to optical measurements of pure CO_2 for that matter) is that in the practice of laser absorption spectroscopy the mole fraction of CO_2 in a gas affects the measured stable isotope ratios (and thus delta values) of CO_2. Quantification, let alone elimination of this CO_2 mole fraction dependence (CMFD) is difficult (McManus et al., 2015), but two sources of CMFD were identified by Wen et al. (2013) and related to different calibration strategies. In the first place, CMFD results from non-ideal fitting of the absorption spectra which will to some extent always occur. Capturing the true absorption spectrum is very complicated, due to among others line broadening effects of the various components of the air, far wing overlap of distant but strong absorptions, and temperature and pressure variability. Secondly, a more "trivial" CMFD is introduced when calibration is done on measured isotopologue ratios and the intercepts of the relation between the isotopologues and the CO_2 mole fraction is non-zero (Griffith et al., 2012). This effect can be explained by

https://doi.org/10.5194/amt-2020-365
Preprint. Discussion started: 12 November 2020
© Author(s) 2020. CC BY 4.0 License.

Atmospheric Measurement Techniques Discussions

expressing the calculation of the isotopologue ratio by:

$$r* = \frac{X_*}{X_{626}} \tag{2}$$

In which X_* is the measured isotopologue mole fraction and * indicates which of the rare isotopologues is used. When the relation of measured isotopologue mole fraction and the CO_2 mole fraction is linear, this can be described by:

$$X_* = X_{CO2} * a + b \tag{3}$$

If equation 2 is then brought into equation 1 for both the rare and the abundant isotopologue mole fraction, and b is non-zero for one of those, a nonlinear CMFD is introduced for which correction is necessary.

3.1.1 Experiment description

Three experiments have been conducted over the last two years to determine the CMFD and to assess its stability over time. These experiments were conducted in December 2017 (experiment 1), in December 2018 (experiment 2) and in May 2019 (experiment 3). Experiment 1 has been conducted in cooperation with the Institute for Marine and Atmospheric research Utrecht (IMAU) and served as the initial determination of the CMFD on the SICAS. Experiments 2 and 3 were meant to assess the stability of the CMFD over time. A methodology to determine the CMFD of the r^{636} for a comparable dual-laser instrument has been described by McManus et al. (2015). In their study, a pure CO_2 working gas was diluted back to different CO_2 mole fractions using a set-up including computer controlled valves connected to a flow of air without CO_2 ("zero-air"). CO_2 and zero-air mixtures were led directly into the continuous flow dual laser instrument. In this way it was possible to measure the CMFD over a wide range of CO_2 mole fractions, from $\sim$0 to 1000 ppm. The CMFD correction function for the isotope ratios was derived by applying a fourth order polynomial fit to these measurements.

For determination of the CMFD on the SICAS this approach was used with some adjustments. The SICAS is designed for the measurement of atmospheric samples of which the relevant range of CO_2 mole fractions is $\sim$370 – 500 ppm, and experiments were therefore for the most part conducted in this range. The SICAS measures discrete air samples, hence air mixtures were manually prepared in sample flasks by back-diluting a well-known pure CO_2 reference gas to different CO_2 molar fractions in the ambient range. Air samples for experiment 1 were prepared at the IMAU, Utrecht University.

Air samples for experiment 2 and 3 were prepared in our own laboratory. The pure CO_2 aliquots were prepared by connecting a 20 mL flask containing a pure CO_2 local reference gas to a calibrated adjustable volume. The required amount of CO_2 in the adjustable volume could be determined by measuring the pressure at a resolution of 1 mBar using a pressure sensor (Keller LEO 2). Both the sample flask and adjustable volume were connected to a vacuum ($3.3*10^{-5}$ mBar) glass line. The CO_2 in the adjustable volume was transferred cryogenically (using liquid nitrogen) into a small glass tube shape attachment on the side of the evacuated sample flask which was custom-made for this purpose and subsequently the zero-air dilutor gas was added. The dilutor gas consists of natural air scrubbed of CO_2 and H_2O using Ascarite® (sodium hydroxide coated silica, Sigma-Aldrich) and Sicapent® (phosphoric anhydride, phosphorus(V) oxide), which results in dry, CO_2-free natural air. For experiment 2, additional samples were prepared using synthetic air mixtures with and without 1% Argon as dilutor gas for evaluation of the effect of air composition on the CMFD (see also section 3.1.6).

https://doi.org/10.5194/amt-2020-365
Preprint. Discussion started: 12 November 2020
© Author(s) 2020. CC BY 4.0 License.

Atmospheric Measurement Techniques Discussions

After closing the flask, the mixture was put to rest for at least one night before measurement to ensure the CO_2 and the dilutor were completely mixed. With our manual preparation system we were able to prepare 10, 12 (with dilutor being whole air) and 7 flasks for experiment 1, 2 and 3 respectively, that were within our relevant range of atmospheric CO_2 mole fractions. McManus et al. (2015) applied a polynomial curve fit on the isotope ratio as a function of the CO_2 mole fraction. In this study we focus on a narrower range of CO_2 mole fractions and therefore we expect that a linear or quadratic relationship is sufficient to describe the measured ratios as a function of the CO_2 mole fraction. We therefore considered the lower number of samples that were used for the three experiments in comparison to the continuous flow experiment by McManus et al. (2015) to be sufficient.

In the next two paragraphs we will discuss the results of the above described experiments for evaluation of the two sources of CMFD according to Wen et al. (2013) for the SICAS.

3.1.2 Non-linearities of measured isotopologues

The first source described by Wen et al. (2013), non-linearity of the relation between the measured isotopologue mole fraction and the CO_2 mole fraction, is determined by analysis of the linear fits of the measured rare isotopologue mole fractions (X_{636}, X_{628} and X_{627}) as a function of the measured X_{626}. We used the $M_{S(t)dc}$ from equation 1 for both the rare isotopologue and the abundant isotopologue mole fractions. The CO_2 mole fraction is calculated by multiplying the $X_{626(t)dc}$ by the known CO_2 mole fraction of the working gas. The residuals of the linear fits are manipulated such that residuals of the lowest mole fractions are zero (figure 5). A linear relation would result in residuals scattering around zero, without a pattern, while systematic non-linearities would result in a significant pattern, recurring for the different experiments. From the results in figure 5 we can conclude that non-linearities occur, however, these are only clearly visible in experiment 1 for the X_{636} and the X_{627} isotopologue, and to a lesser degree in experiment 2 for the X_{636} isotopologue. The maximum residuals of both the X_{636} and the X_{627} are highest in experiment 1, which is also the experiment covering the highest range of CO_2 mole fractions. From these experiments we can therefore conclude that non-linearities of the measured rare isotopologue mole fractions and the X_{626} isotopologue occur, but are only significant if the range of CO_2 mole fraction is higher than 100 ppm. For the X_{628} we do not see significant non-linearities, even if the CO_2 mole fraction is much higher than 100 ppm. The maximum residuals of the X_{628} are not influenced by the CO_2 mole fraction, and we therefore conclude that non-linearities are below the level of detection in these experiments.

3.1.3 Introduced dependency on measured delta values

The second source for CMFD, described by Wen et al. (2013), is the introduced dependency on measured isotope ratios if intercepts of the different isotopologues of the analyser's signal are non-zero, or as in our case for some experiments, if different isotopologues of the analyser's signal are non-linear in a different way. In this paragraph we look into the different possibilities to correct for the CMFD of the measured delta's based on observations of the experiments that were described in the section above.

https://doi.org/10.5194/amt-2020-365
Preprint. Discussion started: 12 November 2020
© Author(s) 2020. CC BY 4.0 License.

Atmospheric Measurement Techniques Discussions

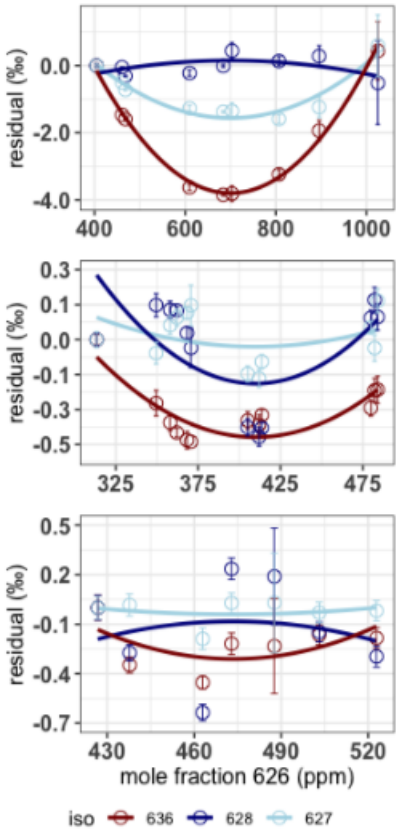

Experiment 1

iso	R^2	max. res
636	0.99	3.85
628	0.34	0.52
627	0.92	1.59

404-1025 ppm

Experiment 2

iso	R^2	max. res
636	0.73	0.43
628	0.39	0.42
627	0.11	0.17

313-484 ppm

Experiment 3

iso	R^2	max. res
636	0.32	0.45
628	0.03	0.64
627	0.05	0.19

426-522 ppm

Figure 5. Residuals of the linear fit of the rare isotopologue abundancies as a function of the X_{626} and the quadratic fit on the residuals. From top to bottom: Experiment 1, experiment 2 and experiment 3. The colours red, darkblue and lightblue are used for the isotopologues 636, 628 and 627 respectively. Error bars are the combined standard deviations of the 626 and rare isotopologue measurements. Per isotopologue the R^2 of the quadratic fit on the residuals is indicated in the tables on the right, as well as the maximum residual (in ‰) on the linear fit of the rare isotopologue as a function of the X_{626}.

https://doi.org/10.5194/amt-2020-365
Preprint. Discussion started: 12 November 2020
© Author(s) 2020. CC BY 4.0 License.

Atmospheric Measurement Techniques Discussions

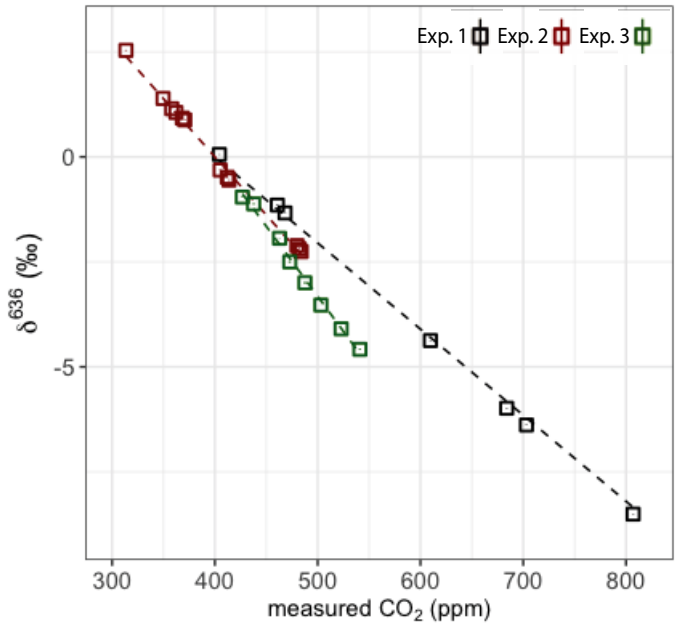

Figure 6. Measured r^{636} of three experiments, black points are experiment 1, red points are experiment 2, green points are experiment 3.

Isotope ratios are susceptible to instrumental drift, but delta values are drift corrected as the uncalibrated delta value δ_{SRaw} is calculated by:

$$\delta_S^* = (\frac{r_S^*}{r_{WG}^*} - 1) \tag{4}$$

Where S and WG stand for sample and working gas respectively and * stands for the rare isotopologue of which the delta is calculated. From now on we use the δ with an isotopologue superscript for uncalibrated delta values, the δ values with an isotope superscript are reserved for calibrated (on the VPDB scale) values. The CMFD's of the delta's are determined by conducting a linear fit on the measured delta values as a function of the measured CO_2 mole fraction.

The results for δ^{636} are shown in figure 6 and slopes of all delta's and the standard errors of the slopes are shown in table 2. Note that in some cases the standard error of the slope is close to the slope itself and it is therefore questionable whether a significant CMFD is measured at all. As measurements were not conducted on CO_2 of similar isotope composition, the δ^{636} measurements in figure 6 were normalized such, that at the CO_2 mole fraction of 400 ppm all ratios are 1. Only the calculated slope is therefore of importance when considering the CMFD of the different experiments. From table 2 it is clear that the δ^{636} shows the strongest CMFD. The results show that the CMFD varies for the three different experiments for all measured delta's. Changing instrumental conditions can be an explanation for this change in the CMFD. A drop in measured laser intensity, for instance, was observed over the period between experiment 1 and expermient 3. We should, however, also consider the different range of CO_2 mole fractions of the different experiments.

https://doi.org/10.5194/amt-2020-365
Preprint. Discussion started: 12 November 2020
© Author(s) 2020. CC BY 4.0 License.

Atmospheric Measurement Techniques Discussions

all values	δ^{636}		δ^{628}		δ^{627}	
in ‰/ppm	slope	se	slope	se	slope	se
exp. 1	-0.0205	0.0003	-0.0013	0.0003	-0.0040	0.0004
exp. 2	-0.0277	0.0006	-0.0027	0.0012	0.0029	0.0007
exp. 3	-0.0333	0.0011	-0.004	0.003	-0.0022	0.0005

Table 2. Slopes derived from the linear fits of the measured delta's and CO_2 mole fractions and the standard errors of the slopes.

all values in ‰		δ^{636}	δ^{628}	δ^{627}
exp.1 (404-1025ppm)	lin	0.871	0.120	0.376
	q	0.072	0.142	0.100
	fit lin	0.141	0.090	0.169
	fit q	0.034	0.092	0.078
exp. 2 (313-484ppm)	lin	0.095	0.181	0.095
	q	0.054	0.164	0.097
	fit lin	0.086	0.175	0.093
	fit q	0.049	0.155	0.093
exp. 3 (426-522ppm)	lin	0.075	0.186	0.048
	q	0.084	0.162	0.032
	fit lin	0.093	0.191	0.037
	fit q	0.082	0.161	0.028

Table 3. Mean residuals for correction of the CMFD of measured ratios using 3 different scenarios; lin is calculated relation assuming linear CMFD of the rare isotopologue mole fraction, q is calculated relation assuming quadratic CMFD of the rare isotopologue mole fraction and fit is a linear fit of the CMFD of the measured isotope ratios. The minimum and maximum CO_2 mole fractions that were used per experiment are shown in the first column.

Although most of the variance occurring in the observed CMFD of the delta's (especially of the δ^{636}) can be explained by the linear relationship we found with the measured CO_2 mole fraction, we can, from the observed non-linearities of the measured isotopologues, expect that these relations are better explained by a polynomial relation. We compare therefore both linear and quadratic fits of the measured delta's with calculated relations derived from the fits of the rare isotopologues as a function of the measured CO_2 mole fraction. Two relations are calculated: assuming a linear CMFD and a quadratic CMFD of the rare isotopologues. To compare all four scenarios (assuming a linear or quadratic CMFD of the measured delta's and calculation of the CMFD of the delta's assuming a linear and a quadratic CMFD of the rare isotopologues) the mean of the absolute residuals of the observations was calculated for all three experiments and shown in table 3. The quadratic fit of the delta's (fit q) shows the lowest mean residuals (except the $\delta^{13}C$ in experiment 3), followed by the calculated relation of the delta's when using a quadratic relation of the individual isotopologues and the CO_2 mole fraction (q). From these results

https://doi.org/10.5194/amt-2020-365
Preprint. Discussion started: 12 November 2020
© Author(s) 2020. CC BY 4.0 License.

Atmospheric Measurement Techniques Discussions

it can therefore be concluded that determination of the quadratic CMFD of the delta's will give the most accurate results in most cases. It is, however, the question whether this is feasible in practice, as we also know that the CMFD can change through time due to changing instrumental conditions. Determination of a (accurate) quadratic relation requires at least three measurement points (but preferably more) of atm-CO_2 of the same isotope composition. In our lab CO_2 in air samples of the same isotope composition but deviating CO_2 mole fractions are prepared manually, introducing again uncertainties, and doing these experiments regularly is therefore labor- and time intensive. Note as well that the range of the CO_2 molar fractions in the 3 experiments is quite high, considering the range of CO_2 molar fractions in atmospheric samples. The differences between the four scenarios are significantly smaller in experiment 3 (covering 96 ppm) than in experiment 1 (covering 621 ppm). In the daily procedure of the SICAS there are at least two reference cylinders measured bracketing most of the CO_2 molar fractions (covering 82 ppm) that occur in atmospheric samples. As all sample and reference measurements are divided by measurements of the working gas when the delta values are calculated, the measured delta value of the working gas should always be zero. The two reference cylinders, together with the zero point for the working gas provide us with three points to determine a quadratic CMFD of the measured delta's. In this way it is possible to apply a quadratic CMFD correction on the measured delta's. It should be noted that tests showed that the improvements of a quadratic fit (in this form) compared to a linear fit were very small within the narrow range of CO_2 molar fractions occurring in the atmosphere, in line with the results of table 3. However, when samples of very deviating CO_2 molar fractions are measured, a quadratic fit will certainly improve the accuracy of the measurement.

3.2 Standard materials and reference scales

Four gas tanks (40 L Luxfer aluminum, alloy 6061, max. pressure of 200 Bars) are used in the daily measurement procedure of the SICAS: a working gas tank used for drift correction and possibly for a first calibration step (WG); a quality control tank that is being treated as a sample (QC); and two tanks that are specifically used for CMFD corrections. These latter two consist of a high mole fraction reference tank (HR) and a low mole fraction reference tank (LR) covering a great part of the CO_2 mole fraction range occurring in atmospheric samples. It is known that with cavity ring down spectroscopy the composition of the sample air affects the absorption line profiles by pressure broadening effects ("matrix effects"), with non-negligible consequences (Nakamichi et al., 2006; Nara et al., 2012). Hence, it is likely that air composition affects CO_2 measurements of absorption spectroscopy in the mid-infrared as well. The possible effects of air composition on the CMFD have been tested by measurement of samples of the same CO_2, mixed to different CO_2 mole fractions, prepared according to the method described in section 3.1.1 using three different dilutor gases. The gaes that have been used in addition to the CO_2 free natural air (whole air), were synthetic air (20% O_2 and 80% N_2, purity is $<= 99.99\%$) and the same synthetic air with addition of 1% of Argon, both prepared by Linde Gas. Linear fits on the measured r^{636} as a function of the CO_2 mole fraction show a small but significant difference of the resulting slopes of 0.0014‰ per ppm (table 4) between the synthetic air and whole air samples. For the r^{628} and r^{627} the slope was much smaller and the standard error of the slope was too large to determine a significant difference between the use of the synthetic dilutors and whole air. Nevertheless, to avoid inaccuracies due to a different CMFD

https://doi.org/10.5194/amt-2020-365
Preprint. Discussion started: 12 November 2020
© Author(s) 2020. CC BY 4.0 License.

Atmospheric Measurement Techniques Discussions

of r^{636} of samples and references, we solely use gas consisting of natural, dried air as then the effects of the (very small) variability in air composition are negligible.

dilutor gas	slope (‰ per ppm)	se. slope (‰)
whole air	-0.0272	0.0006
synthetic air+Ar.	-0.0265	0.0008
synthetic air	-0.0258	0.0007

Table 4. CMFD for samples of the same CO_2 diluted back with different dilutors. Per dilutor the slopes, resulting from the linear fits of measured r^{636} and 626 isotopologue mole fraction (ppm), and the standard errors of the slopes are indicated.

The gas tanks were produced in-house from dry compressed natural air collected at the roof of our institute using a RIX compressor (model SA-3). The HR and LR were produced as follows: the HR cylinder was filled up to ~ 150 Bars in winter at the 15^{th} of January 2018, so the resulting CO_2 mole fraction is relatively high (423.77 ± 0.01 ppm). The LR cylinder was subsequently produced by transferring air from the HR to an empty cylinder, using the pressure difference, while completely removing CO_2 from the air as it flew through a tube filled with Ascarite®. After the LR cylinder was filled up to 13 Bars with CO_2 free air, the Ascarite® filled tube was removed and the filling was continued until the pressure of both cylinders was $\sim$ 70Bars. In this way the CO_2 mole fraction of the LR cylinder was reduced in comparison with the HR cylinder, without influencing the CO_2 isotope ratios. The resulting CO_2 mole fraction of the LR was 342.81$\pm$0.01 ppm. A scheme of the whole set-up and detailed description of the procedure can be found in Appendix B.

Aliquots of all four tanks have been analyzed at the MPI-BGC in Jena by IRMS to link the $\delta^{13}C$ and $\delta^{18}O$ directly to the JRAS-06 scale (Jena Reference Air Set for isotope measurements of CO_2 in air (VPDB/VPDB-CO_2 scale)) (Wendeberg et al., 2013). The JRAS-06 scale uses calcites mixed into CO_2-free whole air to link isotope measurements of atm-CO_2 to the VPDB scale. An overview of our calibration gases measured at the MPI-BGC and their final propagated error is presented in table 5 and it can be seen that the LR and HR are very close in isotope composition but seem to differ slightly in their $\delta^{13}C$ composition (by 0.05‰). Note that the aliquots were prepared using the 'sausage' method, meaning that several (in this case 5) flasks are connected and flushed with the sample gas, resulting in a similar air sample in all flasks. However, deviations of the sampled air and the air in reference cylinders due to small leakages or other gas handling problems might be introduced.

3.3 Calibration methods

We developed two different calibration strategies based on the two main approaches for calibration of isotope measurements, as also described by Griffith et al. (2012), being (1) determine the isotopologue ratios, and calibrate those, taking the introduced CMFD into account, from now on defined as the ratio method (RM), and (2) first calibrate the absolute isotopologue mole fractions individually and then calculate the isotopologue ratios, from now on defined as the isotopologue method (IM). In the following sections these two methods and the results for the SICAS measurements are described.

https://doi.org/10.5194/amt-2020-365
Preprint. Discussion started: 12 November 2020
© Author(s) 2020. CC BY 4.0 License.

Atmospheric Measurement Techniques Discussions

Tank	CO_2 (ppm)	CO_2_err.	$\delta^{13}C(‰)$	$\delta^{13}C$ st.err.	$\delta^{18}O(‰)$	$\delta^{18}O$ st.err.
WG	405.74	0.10	-8.63	0.02	-4.05	0.03
QC	417.10	0.10	-9.13	0.03	-3.25	0.02
LR	342.81	0.01	-9.40	0.02	-3.65	0.03
HR	424.52	0.01	-9.45	0.02	-3.65	0.05

Table 5. Calibrated whole air working standards used in daily operation of the SICAS measurements. CO_2 measurements were conducted in our lab on a PICARRO G2401 gas mole fraction analyzer and the isotope composition was measured at the MPI-BGC with a MAT-252 Dual-Inlet IRMS.

3.3.1 Ratio method

The RM is very similar to calibration strategies applied by isotope measurements using DI-IRMS (Meijer, 2009) and was also proposed in McManus (2015) for the calibration of a comparable QCL laser instrument for the measurement of multiple isotopologues of carbon dioxide (and water). Measured isotopologue mole fractions are used for the estimation of isotope ratios (equation 1), which are calibrated to the international VPDB-CO_2 scale by measurement of several in-house CO_2-in-air references within the same measurement sequence. One of the references is used both for drift correction and a first calibration step, functioning therefore both as machine working gas and reference, and is measured alternately with the samples to reduce instrumental drift. The uncalibrated delta value δ_{SRaw} is calculated by:

$$\delta^*_{SRaw} = (\frac{r^*_S}{r^*_R} - 1) \tag{5}$$

Where S and R stand for sample and reference respectively. The calibrated $\delta^{13}C$ and $\delta^{18}O$ based on the reference that is used is then derived by:

$$\delta_{SCal} = (1 + \delta_R) * \delta_{SRaw} + \delta_R \tag{6}$$

In which δ_R is the known delta value of the reference on the VPDB-CO_2 scale. The $\delta^{17}O$ value is indirectly determined using an assumed relation between $\delta^{17}O$ and $\delta^{18}O$ (λ) ratio of 0.5229 of the machine working gas, a value measured at high precision by Barkan and Luz (2012) of CO_2 that is equilibrated with water. This relation is expressed as follows:

$$(\frac{r^{17}_S}{r^{17}_R}) = (\frac{r^{18}_S}{r^{18}_R})^{\lambda} \tag{7}$$

The calibrated $\delta^{17}O$ value is therefore determined by applying the following equation:

$$\delta^{17}O_{SCal} = ((1 + \delta^{18}O_R)^{\lambda} - 1) * \delta^{17}O_{SRaw} + ((1 + \delta^{18}O_R)^{\lambda} - 1) \tag{8}$$

Where $\delta^{17}O_{SRaw}$ is the uncalibrated measured delta value of the sample and $\delta^{18}O_R$ is the known $\delta^{18}O$ value of the machine working gas.

Up to this point, the procedures are more or less identical to those for IRMS measurements (but without the here unnecessary 'ion correction' and N_2O correction). CMFD correction is specific for laser absorption spectroscopy and is crucial (as can

https://doi.org/10.5194/amt-2020-365
Preprint. Discussion started: 12 November 2020
© Author(s) 2020. CC BY 4.0 License.

Atmospheric Measurement Techniques Discussions

be concluded from section 3.1.3) to derive accurate measurement results when calibration is done using the isotope ratios. We developed a calibration method based on the idea that including the measurement of two reference gases covering the CO_2 range of the measured samples (in our case LR and HR) enables the correction of the measured isotope ratios. These two reference gases are measured several times throughout the measurement sequence and a quadratic fit of the residuals (measured δ_{SCal} - assigned δ_{VPDB}) including the residual of zero for the working gas measurement as a function of the CO_2 mole fraction is done so the following calibration formula can then be determined:

$$\delta_{VPDB} = \delta_{SCal} - ([CO_2]^2 * a + [CO_2] * b + c) \tag{9}$$

In which a and b are the second and first order coefficients respectively and c is the intercept of the quadratic fit of the residuals and the CO_2 mole fractions of the two reference gases, $[CO_2]$ is the measured CO_2 mole fraction and δ_{VPDB} is the calibrated δ value on the VPDB scale.

Also for the $\delta^{17}O$ values a CMFD correction should be applied, but the $\delta^{17}O$ values of our reference cylinders on the VPDB scale are not known, so we cannot calculate the residuals. At this moment this issue is solved by correcting for the CMFD of the $\delta^{17}O$ already on the uncalibrated delta values (δ^{17}_{SRaw}). The (linear) CMFD is determined from the two uncalibrated delta values of LR and HR, by assuming a similar $\delta^{17}O$ composition of both references. We justify this assumption by concluding that during preparation of LR out of HR no fractionation occurred, as the measured $\delta^{18}O$ composition of the references (table 5) showed no differences.

3.3.2 Isotopologue method

The IM is based on the calibration strategy described by Flores et al. (2017) following methods earlier described by Griffith et al. (2012) and will be briefly explained here for clarity. Basically, the method treats the CO_2 isotopologues as if they were independent species, calibrates their mixing ratios individually, and only then combines the results to build isotope ratios and delta values. The mole fraction (X) of the four most abundant isotopologues of a measured CO_2 sample are determined using two references gases with known CO_2 mole fractions and isotope compositions. The CO_2 mole fractions are chosen such that normally occurring CO_2 mole fractions in atmospheric air are bracketed by the two reference gases. The actual (or assigned) mole fractions (X_a) of the four most abundant isotopologues of the reference gases can be calculated using calculations 1-11 in Flores et al. (2017) which are listed in the Appendix 1. Due to the broad range of CO_2 mole fractions that are covered by the reference gases, measurement of both working standards will enable the calculation of the (linear) relation of the measured mole fraction (X_m) and the X_a, which is the calibration equation. X_m is corrected for instrumental drift using equation 1 and can then be implemented as follows:

$$X_a = c + X_m * d \tag{10}$$

In which c and d are the intercept and slope respectively of the linear fit of X_m as a function of X_a of the reference gases. The resulting X_a's can then again be used to calculate the isotope composition using calculation 1-11 in Appendix 1. As the $\delta^{17}O$

https://doi.org/10.5194/amt-2020-365
Preprint. Discussion started: 12 November 2020
© Author(s) 2020. CC BY 4.0 License.

Atmospheric Measurement Techniques Discussions

of our reference tanks have not been measured, an assumed λ of 0.5229 (Barkan and Luz, 2012), is used for determination of the isotopologue mole fraction of 627. The introduced CMFD due to calibration on measured isotope ratios will not occur with this method, and a CMFD correction is therefore not necessary to yield accurate results.

4 Results and discussion

4.1 Monitoring measurement quality and comparison of calibration methods

To capture the very small signals in time-series of the isotope composition of atm-CO_2 it is crucial to keep track of the instruments' performance over the course of longer measurement periods. Variations in precision and accuracy of the isotope measurements on the SICAS are monitored by measurement of a quality control tank (QC) in every measurement sequence. Since the QC measurement is not used for any correction or calibration procedures it can be considered as a known sample measurement that gives an indication of the overall instrument performance. Based on the WMO compatibility goals required for isotope measurements of atm-CO_2 we categorized (high quality (H), medium quality (M) and low quality (L)) three measurement periods for both the RM and IM. A period is rated as H if both the mean accuracy and the mean precision (expressed as the standard error) of the QC measurements over that period are within the WMO compatibility goals (0.01‰ for $\delta^{13}C$ and 0.05‰ for $\delta^{18}O$ (WMO, 2016)), if the accuracy or precision is within the requirements but the other one is not, it is rated M, if both accuracy and precision do not fulfil the requirements it is rated L. Measurements of the QC done over the period of 20th of November 2019 until the 4th of February 2020 are shown in figure 7 and we assigned three distinct measurement periods based on the quality of the measurements. The mean residuals and standard errors of all QC measurements during the three periods are shown in table 6.

From the results we learn that the RM shows in general better precisions than the IM, while the accuracy of the two methods is more or less similar. The RM performs definitely better, because contrary to IM it has the potential to meet the WMO goal of 0.01‰ for the $\delta^{13}C$ measurements.

	Ratio method		Isotopologue method	
period	$\delta^{13}C$ residual	$\delta^{13}C$ st.error	$\delta^{13}C$ residual	$\delta^{13}C$ st.error
1	0.007	0.009	0.04	0.03
2	0.034	0.013	0.03	0.04
3	0.05	0.02	0.04	0.05
	$\delta^{18}O$ residual	$\delta^{18}O$ st.error	$\delta^{18}O$ residual	$\delta^{18}O$ st.error
1	0.016	0.008	0.02	0.03
2	0.050	0.009	0.06	0.04
3	0.048	0.009	0.05	0.04

Table 6. Mean residuals and standard errors of the QC measurements in the three different measurement periods.

https://doi.org/10.5194/amt-2020-365
Preprint. Discussion started: 12 November 2020
© Author(s) 2020. CC BY 4.0 License.

Atmospheric Measurement Techniques Discussions

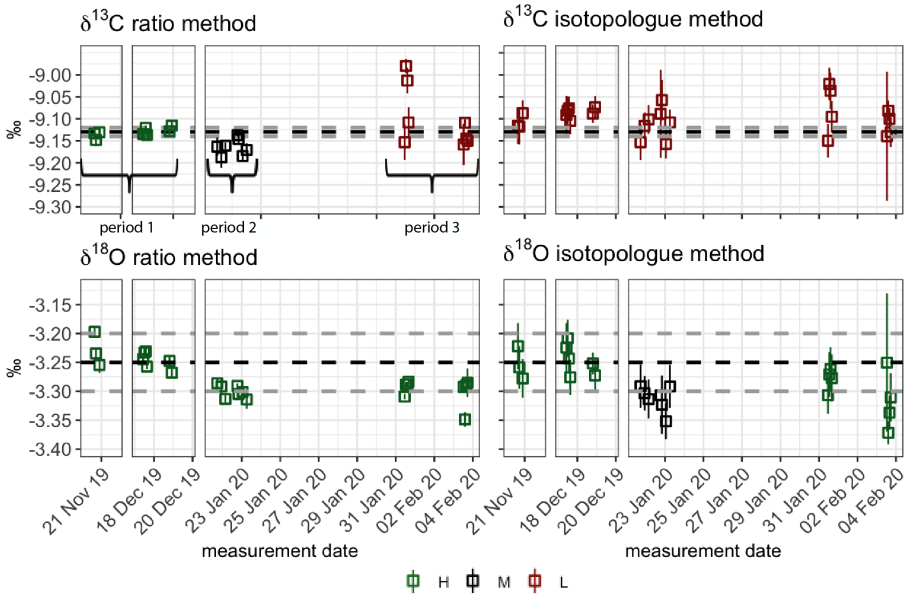

Figure 7. QC $\delta^{13}C$ (upper panels) and $\delta^{18}O$ (lower panels) measurements for both the RM (left) and IM (right). The assigned value of the QC is indicated by the black dotted line and the WMO compatibility goals are indicated by the grey dotted lines. The error bars show the standard error of the measurements. Colour of the points indicates whether the measurements were performed in a H (green), M (black) or L (red) measurement period.

4.2 Intercomparison flask measurements

To test the accuracy of SICAS flask measurements over a wide range of CO_2 mixing ratios, as well as testing the lab compatibility of the SICAS measurements, we measured flask samples that are part of an ongoing lab intercomparison of atmospheric trace gas measurements including the $\delta^{13}C$ and $\delta^{18}O$ of CO_2 (Levin et al., 2004). The sausage flask Intercomparison Program (from now on defined as ICP) has provided since 2002 every 2 to 3 months (occasionally longer periods) aliquots of three high pressure cylinders containing natural air covering a CO_2 mixing ratio range of 340-450 ppm. Participating laboratories send 6 flasks to the ICOS-CAL lab in Jena where these are filled with air from the three cylinders (two flasks per cylinder) with the so called 'sausage method'. The ICP provides therefore the opportunity to compare flask measurements on the SICAS with IRMS flask measurements of the MPI-BGC and other groups. We measured sausage series 90-94, which were filled between April 2018 and January 2020, on the SICAS and calibrated the isotope measurements both with the RM and the IM. SICAS measurements all took place in 2020, with the consequence that the storage of the flasks varies between 3 and 20 months. To place these results in context of intercomparison results of well established isotope and measurement laboratories the ICP results of the Earth System Research Laboratory of the National Oceanic and Atmospheric Administration (NOAA) were also compared to the MPI-BGC results for the same sausage series. The lab-inter-comparison is presented in the usual way: the mean and standard deviation of the differences between our SICAS $\delta^{13}C$ and $\delta^{18}O$ results (both RM and IM calibrated) and

https://doi.org/10.5194/amt-2020-365
Preprint. Discussion started: 12 November 2020
© Author(s) 2020. CC BY 4.0 License.

Atmospheric Measurement Techniques Discussions

		$\delta^{13}C$		$\delta^{18}O$	
		mean	st. dev.	mean	st. dev.
SICAS - MPI-BGC	RM	0.002	0.063	-0.643	0.809
	IM	0.032	0.112	-0.639	0.812
NOAA - MPI-BGC		-0.007	0.074	0.130	0.078

Table 7. Lab intercomparison of ICP sausage 90-94 results. Differences between the SICAS, of both calibration methods, as well as the NOAA IRMS results and the MPI-BGC IRMS results are shown. The mean difference as well as the standard deviation of the differences of the $\delta^{13}C$ and $\delta^{18}O$ are shown.

the MPI-BGC ones are shown in table 7, along with the NOAA-MPI-BGC differences. From this comparison it can be concluded that $\delta^{13}C$ results from the SICAS calibrated with the RM are of similar quality as the MPI-BGC and the NOAA results. The mean of the differences is virtually zero, while the standard deviations of the differences are 0.063 and 0.074‰ for the SICAS and NOAA results respectively. The SICAS results calibrated with the IM show an offset with MPI-BGC of 0.032‰ and a standard deviation of the differences of 0.112‰, so it can be concluded that the IM is performing worse compared to the RM in this lab-intercompatibility analysis.

When we compare the $\delta^{18}O$ measurements, we find that the SICAS results were consequently significantly more depleted with an average difference of -0.64‰ compared to the MPI-BGC results and that the differences vary strongly with a standard deviation of 0.809‰. $\delta^{18}O$ results of the ICP program show in general a larger scatter among the labs than $\delta^{13}C$ results (Levin et al., 2004), as is also visible in table 7 for the NOAA-MPI-BGC difference. The differences between the SICAS- and the MPI-BGC results, however, are far larger than those (or than in fact all differences in the ICP programme). The reason for this too depleted signal is presumably equilibration of CO_2 with water molecules on the glass surface inside the CIO-type sample flasks during storage. Earlier (unpublished) results from our CO_2 extraction system indicated that the water content of our dried atmospheric air samples increased as a function of time inside the flasks. Our atmospheric samples are stored at atmospheric pressure or lower (down to 800 mbar) when part of the sample has been consumed by different measurement devices. The CIO flasks are sealed with two Louwers-Hapert valves and Viton O-rings of which it is known that permeation of water vapour (as well as other gases) occurs over time (Sturm et al., 2004). Both the pressure gradient and the water vapour gradient between the lab atmosphere and the dry sample air inside the flask lead to permeation of water molecules through the valve seals. To check this hypothesis an experiment was conducted in which CIO flasks were filled with air from the QC tank and were measured the same day of the filling procedure and one week and three months later (see table 8). The results show no significant change in the $\delta^{13}C$, while for the $\delta^{18}O$ there is a strong depletion of the flask measurements after 3 months, deviating more than -0.2‰ in comparison to the cylinder measurements. After 1 week there is no change in the $\delta^{18}O$, indicating that depletion of the $\delta^{18}O$ in the CIO flasks occurs over longer time periods. As the flasks from the ICP were measured at the SICAS after relatively long storage times, sometimes longer than two years, this is likely the explanation of the too depleted values in comparison to the MPI-BGC results. A depletion twice as small as for $\delta^{18}O$ is observed in the $\delta^{17}O$ values, as one would expect for a λ

https://doi.org/10.5194/amt-2020-365
Preprint. Discussion started: 12 November 2020
© Author(s) 2020. CC BY 4.0 License.

Atmospheric Measurement Techniques Discussions

of 0.5229. Further investigations about the changing oxygen isotope signal in CIO-sample flasks are being conducted with the aim to be able to make reliable assessments on the quality of $\delta^{18}O$ and $\delta^{17}O$ flasks measurements on the SICAS.

Storage time	Flasks						
	$\delta^{13}C$	std.	$\delta^{18}O$	std.	$\delta^{17}O$	std.	n
1 day	-9.177	0.023	-3.336	0.002	-1.835	0.011	2
1 week	-9.137	0.036	-3.312	0.012	-1.854	0.011	2
3 months	-9.191	0.019	-3.514	0.122	-1.920	0.041	4
	Cylinder						
1 day	-9.178	0.024	-3.332	0.009	-1.854	0.017	4
1 week	-9.160	0.023	-3.299	0.009	-1.857	0.024	3
3 months	-9.180	0.020	-3.299	0.028	-1.893	0.011	4

Table 8. Results of isotope measurements of QC cylinder and QC air in flasks (calibrated with the RM) at different periods after the flask filling procedure. The last column shows the number of cylinder measurements or the number of flasks that were used to calculate the average and the standard deviation.

To check the performance of the SICAS for both the IM and RM over the wide CO_2 range that is covered by the ICP sausage samples, the differences between the MPI-BGC and the SICAS results are plotted in figure 8 against the measured CO_2 mole fraction. Shown is that for both methods the highest differences are seen at the higher end of the CO_2 mole fraction range close to 440ppm, and therefore far out of the range that is covered by the HR and LR cylinders (343-425ppm). Extrapolation of the calibration methods outside the CO_2 mole fraction range of the reference cylinders yields worse compatibility with MPI-BGC, possibly due to the non-linear character of both the isotopologue CO_2 dependency and the ratio CO_2 dependency. It should therefore be concluded that, to achieve highly accurate results of isotope measurements over the whole range of CO_2 mole fractions found in atmospheric samples, the range covered by the reference cylinders would ideally be changed to 380-450 ppm. In the figure we thereby observe that the IM results within the range of 340-425ppm show too heavy values in comparison to the MPI-BGC results. The IM is more susceptible to offsets due to the use of the absolute CO_2 mole fraction of the reference tanks. The uncertainty in the measured CO_2 mole fractions of the reference cylinders, in combination with uncertainties in the measured isotope values is therefore likely the explanation for the higher offsets of the IM results.

4.3 Potential of SICAS $\Delta^{17}O$ measurements for atmospheric research

With the direct measurement of $\delta^{17}O$ in addition to $\delta^{18}O$ (triple oxygen isotope composition) of atm-CO_2, the $\delta^{17}O$ excess ($\Delta^{17}O$) can be calculated. $\Delta^{17}O$ measurements can be a tracer for biosphere activity (Hoag et al., 2005), atmospheric circulation patterns (Mrozek et al., 2016) and different combustion processes (Horváth et al., 2012). The $\Delta^{17}O$ is usually defined as:

$$\Delta^{17}O = ln(1+\delta^{17}O) - \lambda * ln(1+\delta^{18}O) \quad (11)$$

https://doi.org/10.5194/amt-2020-365
Preprint. Discussion started: 12 November 2020
© Author(s) 2020. CC BY 4.0 License.

Atmospheric Measurement Techniques Discussions

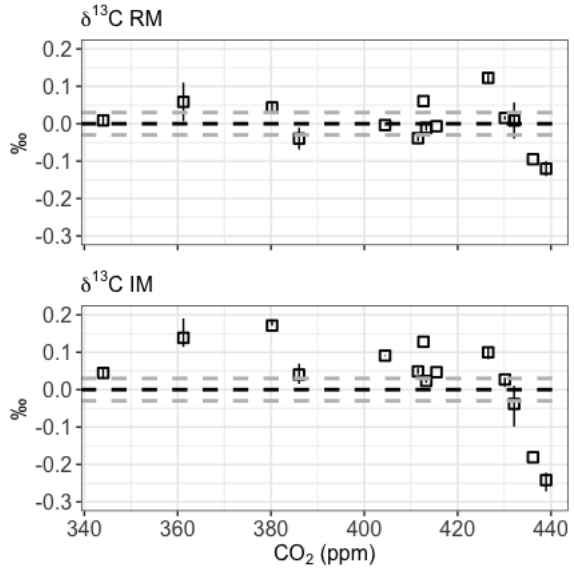

Figure 8. Results of the intercomparison of $\delta^{13}C$ measurements on the SICAS and on the IRMS facility at the MPI-BGC for both the RM (upper) and IM (lower). The MPI-BGC results were subtracted from the SICAS results, the error bars show the standard deviation of the SICAS measurements if more than one aliquot was measured. The grey dotted lines show the 0.03‰ range of residuals.

Variations in the $\Delta^{17}O$ signal in the troposphere are mainly depending on biosphere activity and the influx of stratospheric CO_2 (Koren et al., 2019; Hofmann et al., 2017; Hoag et al., 2005). High measurement precision and accuracy of both the $\delta^{18}O$ and the $\delta^{17}O$ is needed to capture spacial gradients and seasonal cycles in the $\Delta^{17}O$, of which seasonal variations of 0.13‰ (Hofmann et al., 2017) and 0.211‰ (Liang et al., 2017) have been reported. So far it has been an extremely complex and time intensive process to measure $\delta^{17}O$ of CO_2 using DI-IRMS (Hofmann and Pack, 2010; Barkan and Luz, 2012; Mahata et al., 2013; Adnew et al., 2019). Dual-laser absorption spectroscopy as presented in this paper does not require any sample preparation and would therefore be a great step forward in the use of $\Delta^{17}O$ as a tracer for atm-CO_2. Here we present the measurement precision and stability of the $\delta^{17}O$ as well as the $\Delta^{17}O$ measurements of our quality control tank and evaluate the potential for contributing in the field of triple oxygen isotope composition studies.

As our reference cylinders have not been calibrated for their $\delta^{17}O$ values, the evaluation of the $\delta^{17}O$ and $\Delta^{17}O$ measurements of the quality control tank, as shown in figure 9 and table 9, are done based on the mean values and the standard errors of individual measurements over the three measurement periods (as defined in section 4.1), and the stability of the average values during the three periods. The results show good stability of the $\delta^{17}O$ measurements over the first two measurement periods, but in the third period the results for the RM deviate by ~ 0.1‰; those for IM deviate less, about 0.04‰. The precision of the individual $\delta^{17}O$ measurements is similar to the results that were found for the $\delta^{13}C$ and $\delta^{18}O$ measurements of the QC (table 6). The resulting $\Delta^{17}O$ values are less stable over time when calibrated using the RM, with average values ranging from -0.002 to 0.145‰ over the three measurement periods. These deviating values can be explained by the lower measurement quality in

https://doi.org/10.5194/amt-2020-365
Preprint. Discussion started: 12 November 2020
© Author(s) 2020. CC BY 4.0 License.

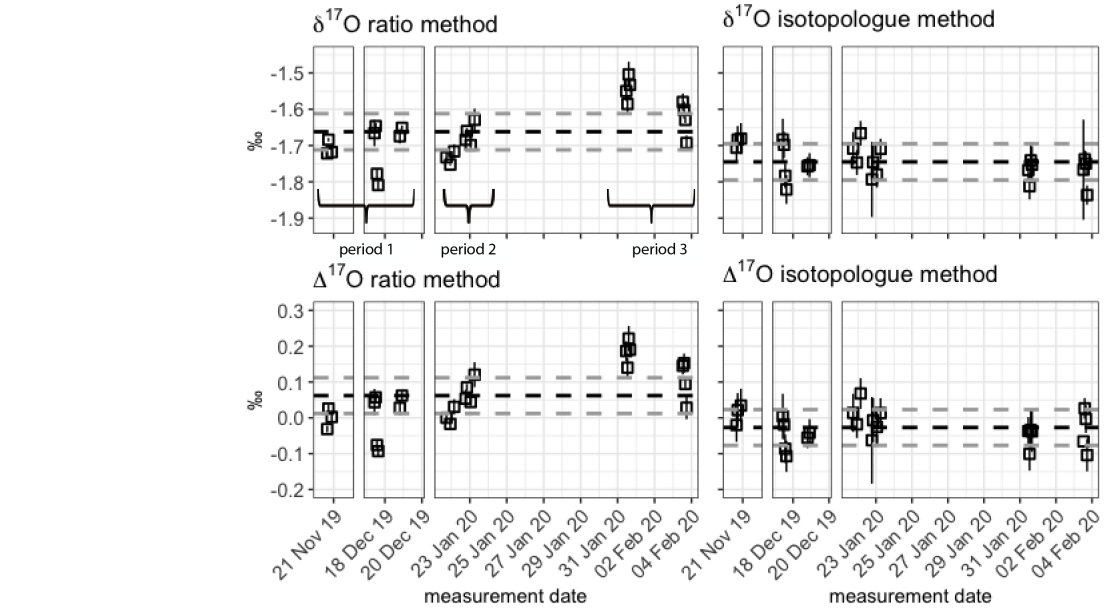

Figure 9. QC $\delta^{17}O$ (upper panels) and $\Delta^{17}O$ (lower panels) measurement averages for the three measurement periods for both the RM (left) and the IM (right). The averages are indicated by the black dotted line and the grey dotted line show the 0.05‰ range around the average. The error bars show the standard error of the measurements.

	Ratio method		Isotopologue method	
period	$\delta^{17}O$ mean	$\delta^{17}O$ st.error	$\delta^{17}O$ mean	$\delta^{17}O$ st. error
1	-1.705	0.013	-1.730	0.038
2	-1.696	0.015	-1.736	0.047
3	-1.585	0.023	-1.770	0.048
	$\Delta^{17}O$ mean	$\Delta^{17}O$ st. error	$\Delta^{17}O$ mean	$\Delta^{17}O$ st. error
1	0.002	0.016	-0.030	0.044
2	0.045	0.019	-0.003	0.057
3	0.145	0.025	-0.045	0.058

Table 9. Average and mean standard error of the QC $\delta^{17}O$ and $\Delta^{17}O$ per measurement period for both the RM and the IM.

https://doi.org/10.5194/amt-2020-365
Preprint. Discussion started: 12 November 2020
© Author(s) 2020. CC BY 4.0 License.

Atmospheric Measurement Techniques Discussions

periods 2 and 3 of the $\delta^{18}O$ measurements, and the strong deviation of the $\delta^{17}O$ value in period 3 compared to period 1 and 2. Values calibrated with the IM show more constant values over the measurement period with average values ranging between -0.045‰ and -0.003‰. Mean standard errors of individual measurements of the three periods are smaller for the RM with a maximum average value of 0.025‰ during period 3, compared to a maximum mean standard error of 0.058‰, also during period 3, for results calibrated using the IM. Due to the lower seasonal variations of the $\Delta^{17}O$ values even higher measurement precisions are a prerequisite and in Hofmann et al. (2017) it is stated that a measurement precision of 0.01‰ or better is required to capture these variations and to use the $\Delta^{17}O$ value as a potential tracer for GPP. These precisions are now not yet achieved, but the results of the RM calibrated values in period 1 show that small improvements in the $\delta^{17}O$ measurements can bring the $\Delta^{17}O$ values close to the 0.01‰ precision. This could for instance be accomplished by deciding to conduct more iterations per measurement, or improvement of the fit stability of laser 1. As the quality of the $\Delta^{17}O$ measurements depends directly on the quality of the the $\delta^{18}O$ and the $\delta^{17}O$ measurements, it will be important to monitor the measurement quality of both isotope values over time using the measurements of the QC tank. In future work we would like to determine the $\delta^{17}O$ VPDB values of our reference cylinders so that the measured $\delta^{17}O$ values can be calibrated using the same method as the $\delta^{13}C$ and the $\delta^{18}O$ measurements.

5 Conclusions and Outlook

In this study we show that WMO compatibility goals can be reached with our Aerodyne dual-laser absorption spectrometer for stable isotope measurements of atm-CO_2 in dry whole air samples if the instrumental conditions are optimal and there is no uncertainty induced because of gas handling procedures (flask sampling for instance). We extensively studied measurement procedures and calibration methods that should be followed to reach these goals. Short-term instrumental drift can effectively be corrected by continuously alternating sample measurements with measurements of a machine working gas. Measuring 10 aliquots of a sample by this method results in standard deviations of the sample measurement ranging between 0.025-0.032‰ and 0.009-0.017‰ for isotopologue and isotope ratio measurements respectively.

Non-linear dependencies on the CO_2 mole fraction occur for measured isotopologue abundances but are insignificant in the typical ambient CO_2 mole fraction range. Measured isotope ratios also show a non-linear CO_2 mole fraction dependency and correction is needed to obtain accurate results of isotope measurements on the SICAS. We observed that CMFD changed through time and therefore using a fixed CMFD correction imposes the risk of inaccurate results when instrumental conditions change. We therefore included at least two reference cylinders in all measurement sequences, covering the range of atmospheric CO_2 mole fractions so CMFD correction can be conducted for each individual batch of samples based on the reference cylinder measurements. To reduce residuals when doing a linear CMFD correction for the non-linear dependencies that were found, using a relevant, and not too high range of CO_2 mole fractions is essential. Due to significant differences found in CMFD between natural air and synthetic mixtures, we used natural air as reference gases (or air mixtures close to natural air).

We tested two calibration methods, of which one is based on measured isotope ratios and a CMFD correction (RM), and one is based on measured isotopologue abundancies (IM). A quality control tank (QC) of known isotope composition is

https://doi.org/10.5194/amt-2020-365
Preprint. Discussion started: 12 November 2020
© Author(s) 2020. CC BY 4.0 License.

Atmospheric Measurement Techniques Discussions

included in all measurement sequences but it is not used for calibration of the samples, which gives the opportunity to study the performance of measurement stability and precision over longer periods. From studying the results of the QC we conclude that precisions are significantly better for the RM, while measurement stability is very similar, both for the $\delta^{13}C$ and the $\delta^{18}O$ measurements. These QC measurements give insight into the overall measurement quality of measurements performed in a certain period. In this way we will be able to evaluate whether measurements conducted in a certain period comply with WMO compatibility goals and we can detect problems with the instrument or reference cylinders in an early stage.

A comparison of SICAS results for both calibration methods with results from the MPI-BGC using flask measurements from the sausage ICP show that the RM performs significantly better for accuracies of $\delta^{13}C$ over a wide CO_2 range than the IM. We found that $\delta^{18}O$ measurements were consequently too depleted due to too long storage times of the CIO flasks before measurement. Future investigations will give more insight in the stability of the oxygen isotopes within the CIO flasks and we will evaluate the possibility of a correction based on storage time.

The SICAS measures the $\delta^{17}O$ with similar precision and stability as the $\delta^{18}O$ and the $\delta^{13}C$ and, although more susceptible to measurement instabilities due to the dependency of the measurement quality of three oxygen isotopes, the results for the $\Delta^{17}O$ are promising. Precisions during periods of optimal measurement quality are now 0.016‰, close to the required measurement precision of 0.01‰ for capturing seasonal variations in the $\Delta^{17}O$ signal. Improvements in the stability of the fit and increasing the number of measurements per sample are considered to improve measurement precisions of the $\Delta^{17}O$ results.

Data availability. All data that has been used for this study which was measured at the SICAS can be found in the supplementary material.

Appendix A: Equations for calculation of isotopologue mole fractions

Individual isotopologues of standards of known CO_2 mole fractions and isotope composition are calculated for the IM calibration method by the equations below, according to Flores et al. (2017), starting with equations for the atomic abundances X in each of the calibration gas mixtures (A1-A5):

$$X(^{12}C) = \frac{1}{1+R^{13}} \tag{A1}$$

$$X(^{13}C) = \frac{R^{13}}{1+R^{13}} \tag{A2}$$

$$X(^{16}O) = \frac{1}{1+R^{18}+R^{17}} \tag{A3}$$

$$X(^{17}O) = \frac{R^{17}}{1+R^{18}+R^{17}} \tag{A4}$$

https://doi.org/10.5194/amt-2020-365
Preprint. Discussion started: 12 November 2020
© Author(s) 2020. CC BY 4.0 License.

Atmospheric Measurement Techniques Discussions

$$X(^{18}O) = \frac{R^{18}}{1 + R^{18} + R^{17}} \tag{A5}$$

where

$$R^{13} = R^{13}_{VPDB-CO_2} * (1 + \delta^{13}C) \tag{A6}$$

$$R^{17} = R^{17}_{VPDB-CO_2} * (1 + \delta^{18}O)^{\lambda} \tag{A7}$$

$$R^{18} = R^{18}_{VPDB-CO_2} * (1 + \delta^{18}O) \tag{A8}$$

and $\delta^{13}C$ and $\delta^{18}O$ are the delta values. $R^{13}_{VPDB-CO_2}$ (0.011180), $R^{17}_{VPDB-CO_2}$ (0.0003931) and $R^{18}_{VPDB-CO_2}$ (0.00208835) values were taken from Brand et al. (2010) for $VPDB - CO_2$. Then each carbon dioxide isotopologue mole fraction in the reference gas was calculated according to its composition using equations A9-A10:

$$X_{626} = (X(^{12}C) * X(^{16}O) * X(^{16}O)) * X_{CO_2} \tag{A9}$$

$$X_{636} = (X(^{13}C) * X(^{16}O) * X(^{16}O)) * X_{CO_2} \tag{A10}$$

$$X_{628} = (X(^{12}C) * X(^{16}O) * X(^{18}O)) * 2 * X_{CO_2} \tag{A11}$$

$$X_{627} = (X(^{12}C) * X(^{16}O) * X(^{17}O)) * 2 * X_{CO_2} \tag{A12}$$

For a more elaborated explanation of these equations, see Flores et al. (2017).

Appendix B: Set-up for preparation of LR

Set-up for preparation of LR out of air from HR: HR, filled up to ~150 Bars with dry natural air, is connected to a similar, empty cylinder. Half of the air in HR will be transferred (passive transfer using the pressure difference) into the empty cylinder to produce LR. The CO_2 mole fraction in LR is reduced by leading part of the air over an Ascarite® filled cartridge that removes all CO_2 from the air, so no isotope fractionation will occur. Successively it is led over a magnesium perchlorate filled

https://doi.org/10.5194/amt-2020-365
Preprint. Discussion started: 12 November 2020
© Author(s) 2020. CC BY 4.0 License.

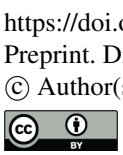

Atmospheric Measurement Techniques Discussions

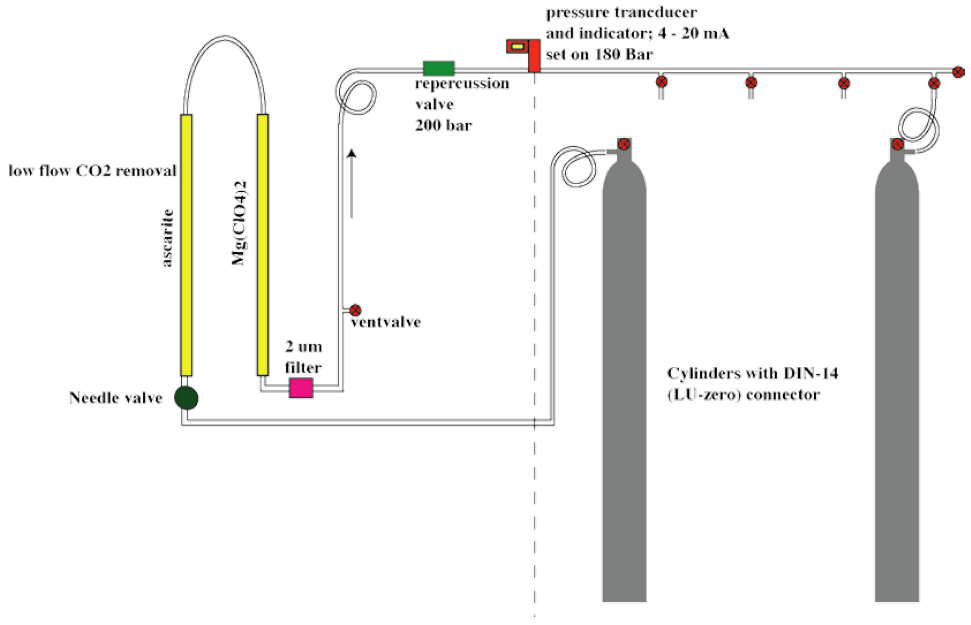

Figure A1.

cartridge to remove water from the air that is potentially stored in the hydrophilic Ascarite®. A needle valve installed before the cartridges creates a low flow to ensure the complete removal of the CO_2 from the air. The pressure sensor installed after the repercussion valve enables to estimate when LR is filled with the amount of CO_2 free air needed to obtain the preferred CO_2 mole fraction. When the preferred amount of CO_2 free air is transferred into the LR cylinder, the cartridges are decoupled from the system to transfer the rest of the air from HR to LR.

Author contributions. P. S., H. S. and H. M. conceived the experiments, which were conducted by P. S. and H. S., P. S. carried out the data-analysis. D. N. and B. M. optimised the fit and contributed with technical assistance for development of the gas handling system as well as solving problems with the instrumentation. The manuscript was written by P. S., H. S. and H. M. contributed with discussions and comments throughout the writing process.

Competing interests. Authors D.N. and B.M. work for Aerodyne Research Inc. which is the company that developed the instrument described in this study.

Acknowledgements. We would like to thank H. M. Moossen, as well as his colleagues at the MPI-BGC, for measuring our reference cylinders and providing us with the data that we required for the intercomparison. We greatly acknowledge the help of G. Adnew from IMAU who

https://doi.org/10.5194/amt-2020-365
Preprint. Discussion started: 12 November 2020
© Author(s) 2020. CC BY 4.0 License.

Atmospheric Measurement Techniques Discussions

prepared the samples for the first CMFD experiment and helped measuring them. We also want to thank M. de Vries, B.A.M. Kers and R. Ritchie for helping us to develop the sampling system as well as the the required software development, and D. Paul for general assistance. This research was partly funded by the European Metrology Programme for Innovation and Research 16ENV06 "Metrology for Stable Isotope Reference Standards (SIRS)".

https://doi.org/10.5194/amt-2020-365
Preprint. Discussion started: 12 November 2020
© Author(s) 2020. CC BY 4.0 License.

Atmospheric Measurement Techniques Discussions

References

Adnew, G. A., Hofmann, M. E., Paul, D., Laskar, A., Surma, J., Albrecht, N., Pack, A., Schwieters, J., Koren, G., Peters, W., and Röckmann, T.: Determination of the triple oxygen and carbon isotopic composition of CO_2 from atomic ion fragments formed in the ion source of the 253 Ultra high-resolution isotope ratio mass spectrometer, Rapid Communications in Mass Spectrometry, 33, 1363–1380, https://doi.org/10.1002/rcm.8478, 2019.

Allison, C. and Francey, R.: High precision stable isotope measurements of atmospheric trace gases, Reference and intercomparison materials for stable isotopes of light elements, IAEA-TECDOC, 131–154, 1995.

Allison, C., Francey, R., and Meijer, H.: Recommendations for the reporting of stable isotope measurements of carbon and oxygen in CO_2 gas, IAEA-TECDOC, 825, 155–162, 1995.

Assonov, S. S. and Brenninkmeijer, C. A. M.: On the ^{17}O correction for CO_2 mass spectrometric isotopic analysis, Rapid Communications in Mass Spectrometry, 17, 1007–1016, https://doi.org/10.1002/rcm.1012, 2003.

Barkan, E. and Luz, B.: High-precision measurements of $^{17}O/^{16}O$ and $^{18}O/^{16}O$ ratios in CO_2, Rapid Communications in Mass Spectrometry, 26, 2733–2738, https://doi.org/10.1002/rcm.6400, http://doi.wiley.com/10.1002/rcm.6400, 2012.

Becker, J. F., Sauke, T. B., and Loewenstein, M.: Stable isotope analysis using tunable diode laser spectroscopy, Applied Optics, 31, 1921–1927, 1992.

Brand, W. A., Assonov, S. S., and Coplen, T. B.: Correction for the ^{17}O interference in $\delta(^{13}C)$ measurements when analyzing CO_2 with stable isotope mass spectrometry (IUPAC Technical Report), Pure and Applied Chemistry, 82, 1719–1733, https://doi.org/10.1351/PAC-REP-09-01-05, https://www.degruyter.com/view/j/pac.2010.82.issue-8/pac-rep-09-01-05/pac-rep-09-01-05.xml, 2010.

Erdélyi, M., Richter, D., and Tittel, F.: $^{13}CO_2/^{12}CO_2$ isotopic ratio measurements using a difference frequency-based sensor operating at 4.35 μm, Applied Physics B: Lasers and Optics, 75, 289–295, https://doi.org/10.1007/s00340-002-0960-2, 2002.

Flores, E., Viallon, J., Moussay, P., Griffith, D. W. T., and Wielgosz, R. I.: Calibration Strategies for FT-IR and Other Isotope Ratio Infrared Spectrometer Instruments for Accurate $\delta^{13}C$ and $\delta^{18}O$ Measurements of CO_2 in Air, Analytical Chemistry, 89, 3648–3655, https://doi.org/10.1021/acs.analchem.6b05063, http://pubs.acs.org/doi/abs/10.1021/acs.analchem.6b05063, 2017.

Gagliardi, G., Castrillo, A., Iannone, R. Q., Kerstel, E. R., and Gianfrani, L.: High-precision determination of the $^{13}CO_2/^{12}CO_2$ isotope ratio using a portable 2.008-μm diode-laser spectrometer, Applied Physics B: Lasers and Optics, 77, 119–124, https://doi.org/10.1007/s00340-003-1240-5, 2003.

Griffith, D. W., Deutscher, N. M., Caldow, C., Kettlewell, G., Riggenbach, M., and Hammer, S.: A Fourier transform infrared trace gas and isotope analyser for atmospheric applications, Atmospheric Measurement Techniques, 5, 2481–2498, https://doi.org/10.5194/amt-5-2481-2012, 2012.

Hoag, K. J., Still, C. J., Fung, I. Y., and Boering, K. A.: Triple oxygen isotope composition of tropospheric carbon dioxide as a tracer of terrestrial gross carbon fluxes, Geophysical Research Letters, 32, 1–5, https://doi.org/10.1029/2004GL021011, 2005.

Hofmann, M. and Pack, A.: Development of a technique for high-precision analysis of triple oxygen isotope ratios in carbon dioxide, Analytical Chemistry, 82, 4357–4361, 2010.

Hofmann, M. E. G., Horváth, B., Schneider, L., Peters, W., Schützenmeister, K., and Pack, A.: Atmospheric measurements of $\Delta^{17}O$ in CO_2 in Göttingen, Germany reveal a seasonal cycle driven by biospheric uptake, Geochimica et Cosmochimica Acta, https://doi.org/10.1016/j.gca.2016.11.019, 2017.

https://doi.org/10.5194/amt-2020-365
Preprint. Discussion started: 12 November 2020
© Author(s) 2020. CC BY 4.0 License.

Atmospheric Measurement Techniques Discussions

Horváth, B., Hofmann, M. E., and Pack, A.: On the triple oxygen isotope composition of carbon dioxide from some combustion processes, Geochimica et Cosmochimica Acta, 95, 160–168, https://doi.org/10.1016/j.gca.2012.07.021, 2012.

IAEA: Stable isotope measurement techniques for atmospheric greenhouse gases, IAEA-TECDOC, 1268, 2002.

IAEA: Reference Sheet: Certified Reference Material : IAEA-603 (calcite) — Stable Isotope Reference Material, https://nucleus.iaea.org/rpst/ReferenceProducts/ReferenceMaterials/Stable{_}Isotopes/13C18and7Li/IAEA-603.htm, 2016.

Kerstel, E. R., Van Trigt, R., Dam, N., Reuss, J., and Meijer, H. A.: Simultaneous determination of the $2^H/1^H$, $^{17}O/^{16}O$, and $^{18}O/^{16}O$ isotope abundance ratios in water by means of laser spectrometry, Analytical Chemistry, 71, 5297–5303, https://doi.org/10.1021/ac990621e, 1999.

Koren, G., Schneider, L., van der Velde, I. R., van Schaik, E., Gromov, S. S., Adnew, G. A., Mrozek Martino, D. J., Hofmann, M. E. G., Liang, M.-C., Mahata, S., Bergamaschi, P., van der Laan-Luijkx, I. T., Krol, M. C., Röckmann, T., and Peters, W.: Global 3-D Simulations of the Triple Oxygen Isotope Signature $\Delta^{17}O$ in Atmospheric CO_2, Journal of Geophysical Research: Atmospheres, 124, 8808–8836, https://doi.org/10.1029/2019jd030387, 2019.

Laskar, A. H., Mahata, S., and Liang, M. C.: Identification of Anthropogenic CO_2 Using Triple Oxygen and Clumped Isotopes, Environmental Science and Technology, 50, 11 806–11 814, https://doi.org/10.1021/acs.est.6b02989, 2016.

Levin, I., Facklam, C., Schmidt, M., Ramonet, M., Ciais, P., Xueref, I., Langenfelds, R., Allison, C., Francey, R., Jordan, A., Rothe, M., Brand, W. A., Neubert, R. E., Meijer, H. A. J., Machida, T., and Mukai, H.: Results of inter-comparison programme for analysis of "sausage" flask air samples, Special report 2, 2004.

Liang, M. C., Mahata, S., Laskar, A. H., and Bhattacharya, S. K.: Spatiotemporal variability of oxygen isotope anomaly in near surface air CO_2 over urban, semi-urban and ocean areas in and around Taiwan, Aerosol and Air Quality Research, 17, 706–720, https://doi.org/10.4209/aaqr.2016.04.0171, 2017.

Luz, B., Barkan, E., and Bender, M. L.: Triple-isotope composition of atmospheric oxygen as a tracer of biosphere productivity, Letters to Nature, 400, 547–550, 1999.

Mahata, S., Bhattacharya, S. K., Wang, C. H., and Liang, M. C.: Oxygen isotope exchange between O_2 and CO_2 over hot platinum: An innovative technique for measuring $\Delta^{17}O$ in CO_2, Analytical Chemistry, 85, 6894–6901, https://doi.org/10.1021/ac4011777, 2013.

McManus, J. B., Nelson, D. D., Shorter, J. H., Jimenez, R., Herndon, S., Saleska, S., and Zahniser, M.: A high precision pulsed quantum cascade laser spectrometer for measurements of stable isotopes of carbon dioxide, Journal of Modern Optics, 52, 2309–2321, https://doi.org/10.1080/09500340500303710, 2005.

McManus, J. B., Nelson, D. D., and Zahniser, M. S.: Design and performance of a dual-laser instrument for multiple isotopologues of carbon dioxide and water, Optics Express, 23, 6569, https://doi.org/10.1364/OE.23.006569, https://www.osapublishing.org/abstract.cfm?URI=oe-23-5-6569, 2015.

Meijer, H. A. J.: Stable isotope quality assurance using the 'Calibrated IRMS' strategy, Isotopes in Environmental and Health Studies, 45, 150–163, https://doi.org/10.1080/10256010902869113, 2009.

Meijer, H. A. J., Neubert, R. E. M., and Visser, G. H.: Cross contamination in dual inlet isotope ratio mass spectrometers, International Journal of Mass Spectrometry, 198, 45–61, https://doi.org/10.1016/S1387-3806(99)00266-3, 2000.

Mrozek, D. J., Van Der Veen, C., Hofmann, M. E., Chen, H., Kivi, R., Heikkinen, P., and Röckmann, T.: Stratospheric Air Sub-sampler (SAS) and its application to analysis of $\Delta^{17}O(CO_2)$ from small air samples collected with an AirCore, Atmospheric Measurement Techniques, 9, 5607–5620, https://doi.org/10.5194/amt-9-5607-2016, 2016.

https://doi.org/10.5194/amt-2020-365
Preprint. Discussion started: 12 November 2020
© Author(s) 2020. CC BY 4.0 License.

Atmospheric Measurement Techniques Discussions

Murnick, D. E. and Peer, B. J.: Laser-based analysis of carbon isotope ratios, Science, 263, 945–947, https://www.jstor.org/stable/2883266, 1994.

Nakamichi, S., Kawaguchi, Y., Fukuda, H., Enami, S., Hashimoto, S., Kawasaki, M., Umekawa, T., Morino, I., Suto, H., and Inoue, G.: Buffer-gas pressure broadening for the (3 0^0 1)$_{III}\leftarrow$ (0 0 0) band of CO_2 measured with continuous-wave cavity ring-down spectroscopy, Chemical Physics, 8, 364–368, https://doi.org/10.1039/B511772K, 2006.

Nara, H., Tanimoto, H., Tohjima, Y., Mukai, H., Nojiri, Y., Katsumata, K., and Rella, C. W.: Effect of air composition (N_2 , O_2 , Ar , and H_2O) on CO_2 and CH_4 measurement by wavelength-scanned cavity ring-down spectroscopy : calibration and measurement strategy, Atmospheric Measurement Techniques, 5, 2689–2701, https://doi.org/10.5194/amt-5-2689-2012, 2012.

Neubert, R. E., Spijkervet, L. L., Schut, J. K., Been, H. A., and Meijer, H. A.: A computer-controlled continuous air drying and flask sampling system, Journal of Atmospheric and Oceanic Technology, 21, 651–659, https://doi.org/10.1175/1520-0426(2004)021<0651:ACCADA>2.0.CO;2, 2004.

Pataki, D. E., Bowling, D. R., and Ehleringer, J. R.: Seasonal cycle of carbon dioxide and its isotopic composition in an urban atmosphere: Anthropogenic and biogenic effects, Journal of Geophysical Research, 108, 4735, https://doi.org/10.1029/2003JD003865, http://doi.wiley.com/10.1029/2003JD003865, 2003.

Roeloffzen, J. C., Mook, W. G., and Keeling, C. D. .: Trend and variations in stable carbon isotopes of atmospheric carbon dioxide, Stable isotopes in plant nutrition, soil fertility and environmental studies, pp. 601–618, 1991.

Rothman, L. S., Gordon, I. E., Babikov, Y., Barbe, A., Chris Benner, D., Bernath, P. F., Birk, M., Bizzocchi, L., Boudon, V., Brown, L. R., Campargue, A., Chance, K., Cohen, E. A., Coudert, L. H., Devi, V. M., Drouin, B. J., Fayt, A., Flaud, J. M., Gamache, R. R., Harrison, J. J., Hartmann, J. M., Hill, C., Hodges, J. T., Jacquemart, D., Jolly, A., Lamouroux, J., Le Roy, R. J., Li, G., Long, D. A., Lyulin, O. M., Mackie, C. J., Massie, S. T., Mikhailenko, S., Müller, H. S., Naumenko, O. V., Nikitin, A. V., Orphal, J., Perevalov, V., Perrin, A., Polovtseva, E. R., Richard, C., Smith, M. A., Starikova, E., Sung, K., Tashkun, S., Tennyson, J., Toon, G. C., Tyuterev, V. G., and Wagner, G.: The HITRAN2012 molecular spectroscopic database, Journal of Quantitative Spectroscopy and Radiative Transfer, 130, 4–50, https://doi.org/10.1016/j.jqsrt.2013.07.002, 2013.

Santrock, J., Studley, S. A., and Hayes, J. M.: Isotopic Analyses Based on the Mass Spectra of Carbon Dioxide, Analytical Chemistry, 57, 1444–1448, https://doi.org/10.1021/ac00284a060, 1985.

Sturm, P., Leuenberger, M., Sirignano, C., Neubert, R. E. M., Meijer, H. A. J., Langenfelds, R., Brand, W. A., and Tohjima, Y.: Permeation of atmospheric gases through polymer O-rings used in flasks for air sampling, Journal of Geophysical Research: Atmospheres, 109, 1–9, https://doi.org/10.1029/2003jd004073, 2004.

Trolier, M., White, J. W., Tans, P. P., Masarie, K. A., and Gemery, P. A.: Monitoring the isotopic composition of atmospheric CO_2: Measurements from the NOAA global air sampling network, Journal of Geophysical Research Atmospheres, 101, 25 897–25 916, https://doi.org/10.1029/96jd02363, 1996.

Tuzson, B., Mohn, J., Zeeman, M. J., Werner, R. A., Eugster, W., Zahniser, M. S., Nelson, D. D., McManus, J. B., and Emmenegger, L.: High precision and continuous field measurements of $\delta^{13}C$ and $\delta^{18}O$ in carbon dioxide with a cryogen-free QCLAS, Applied Physics B: Lasers and Optics, 92, 451–458, https://doi.org/10.1007/s00340-008-3085-4, 2008.

Vogel, F., Huang, L., Ernst, D., Giroux, L., and Worthy, D.: Evaluation of a cavity ring-down spectrometer for in situ observations of $^{13}CO_2$, Atmospheric Measurement Techniques, 6, 301–308, https://doi.org/10.5194/amt-6-301-2013, www.atmos-meas-tech.net/6/301/2013/, 2013.

https://doi.org/10.5194/amt-2020-365
Preprint. Discussion started: 12 November 2020
© Author(s) 2020. CC BY 4.0 License.

Wen, X. F., Meng, Y., Zhang, X. Y., Sun, X. M., and Lee, X.: Evaluating calibration strategies for isotope ratio infrared spectroscopy for atmospheric $^{13}CO_2/^{12}CO_2$ measurement, Atmospheric Measurement Techniques, 6, 1491–1501, https://doi.org/10.5194/amt-6-1491-2013, 2013.

Wendeberg, M., Richter, J. M., Rothe, M., and Brand, W. A.: Jena Reference Air Set (JRAS): A multi-point scale anchor for isotope measurements of CO_2 in air, Atmospheric Measurement Techniques, 6, 817–822, https://doi.org/10.5194/amt-6-817-2013, 2013.

WMO: 18th WMO/IAEA meeting on carbon dioxide, other greenhouse gases and related measurement techniques (GGMT-2015), in: GAW Report, vol. 229, https://library.wmo.int/opac/doc{_}num.php?explnum{_}id=3074, 2016.

Zhou, L., Conway, T. J., White, J. W. C., Mukai, H., Zhang, X., Wen, Y., Li, J., and Macclune, K.: Long-term record of atmospheric CO 2 and stable isotopic ratios at Waliguan Observatory : Background features and possible drivers , 1991 – 2002, 19, 1–9, https://doi.org/10.1029/2004GB002430, 2005.